Auralization of Wind Turbines

Kurt Heutschi, Reto Pieren

Empa, Swiss Federal Laboratories for Materials Science and Technology, Laboratory for Acoustics/Noise Control 8600 Dübendorf, Switzerland, Email: kurt.heutschi@empa.ch

Introduction

The auralization tool presented here is part of the ongoing project VisAsim [1][2][3][4] that will investigate the landscape impact assessment of wind farms considering both visual and acoustical stimuli. It is a collaboration between the Institute for Planning Landscapes and Urban Systems (PLUS) of ETH Zurich and the Laboratory for Acoustics/Noise Control of Empa. The project will end in 2014.
Sounds from modern wind turbines usually consist of broadband noise and possible discrete tonal components [5]. An often reported phenomenon related to wind turbine noise is the periodic amplitude modulation (AM) of the sound pressure level, which is related to the blade passing frequency of the turbine. Besides these periodic modulations there are stochastic fluctuations that have to be considered in an emission synthesizer.
Sound propagation from wind turbines to typical listener positions has the distinction of highly elevated sources and large distances to the receiver. The height of the source strongly reduces the sensitivity of the propagation attenuation with respect to meteorological conditions [6]. However, as wind turbine noise occurs during periods with relative high wind speeds, level fluctuations due to turbulence have to be considered in a propagation filter.

Emission synthesizer

General assumptions and model structure

The emission signal $e(t)$ is supposed to be composed of possible tonal components and broadband noise with frequency dependent, periodic and stochastic amplitude modulation (AM):

$$e(t) = p_{\text{tonal}}(t) + p_{\text{noise}}(t) \tag{1}$$

where p_{noise} is generated by superposition of individually generated third octave band noise signals with appropriate scaling of their levels L_i. As input parameters the model uses four figures per 1/3 octave band plus some general input parameters, such as the blade passing frequency of the turbine. This results in a total number of about 120 input parameters to steer the synthesizer.

Amplitude modulation

The amplitude modulation (AM) is implemented by a time dependent variation of the 1/3 octave band levels $L_i(t)$. The functions $L_i(t)$ are assumed to consist of three additive parts

$$L_i(t) = \overline{L_i} + F_{\text{periodic},i}(t) + F_{\text{stochastic},i}(t) \tag{2}$$

where $\overline{L_i}$ denotes the arithmetic average sound pressure level, $F_{\text{periodic},i}(t)$ is a periodic level fluctuation function representing the periodic AM and $F_{\text{stochastic},i}(t)$ is a stochastic process representing the stochastic AM. $L_i(t)$ is synthesized at a sampling frequency $f_{sL} = 30$ Hz and then upsampled to the audio sampling frequency $f_s = 44.1$ kHz before being applied as amplitude modulation.

Periodic amplitude modulation

The periodic level fluctuation $F_{\text{periodic},i}(t)$ is a periodic function with period $T_{BP} = 1/f_{BP}$. f_{BP} denotes the blade passing frequency (BPF) of the turbine given in Hz and can be calculated from the rotational speed f_{rot} [rpm] of the turbine by $f_{BP} = f_{rot} \cdot N_{\text{blades}}/60$ with the number of blades N_{blades} being typically = 3. With the periodic level fluctuations the well-known "swishing" and "thumping" sounds are implemented. The periodic level fluctuation is a periodic function with a defined amplitude and can be expressed as

$$F_{\text{periodic},i}(t) = s_{\text{periodic},i} \cdot G(t - T_h) \tag{3}$$

with the standard deviation $s_{\text{periodic},i}$ of the periodic level fluctuations in dB and the periodic function G having zero mean and period T_{BP}. Motivated by measured sound pressure level curves and based on listening tests where measured signals were compared to synthetic signals, it was decided to use a triangular waveform for G.

Stochastic amplitude modulation

The stochastic level fluctuations $F_{\text{stochastic},i}(t)$ are generated by random processes. As especially at high frequencies the stochastic level fluctuations between 1/3 octave bands are highly correlated, groups of 1/3 octave bands steered by the same fluctuation function $\eta_j(t)$ are used. For every group j an ARMA model generates a stochastic fluctuation function which is then normalized to unit signal power to obtain the fluctuation signal $\eta_j(t)$. The stochastic level fluctuations are then given by

$$F_{\text{stochastic},i}(t) = s_{\text{stochastic},i} \cdot \eta_j(t) \tag{4}$$

where $s_{\text{stochastic},i}$ is the standard deviation of the stochastic level fluctuations in dB. It has been found that in all cases studied so far, the level fluctuations could be well modelled by a white Gaussian process filtered by a 1st order Butterworth low-pass filter. From about 20 measurements at different wind conditions and different turbine types by means of least squares fits, the following approximation formula for the cutoff frequency $f_{c,j}$ of the low-pass filter in the ARMA process was derived

$$f_{c,j} = \frac{1}{N_{m,j}} \sum_{i \in j} \left[\begin{cases} 10^{0.7 \log(f_{c,i}) - 1.5} \text{ Hz}, & f_{c,i} < 1.6 \text{ kHz} \\ 5 \text{ Hz}, & f_{c,i} \geq 1.6 \text{ kHz} \end{cases} \right] \tag{5}$$

with $N_{m,j}$: number of 1/3 octave bands in group j.

Signal analysis

The synthesizer parameters were determined by analyzing audio recordings taken at the reference position according to IEC61400-11 [7]. For the investigated Vestas V90 and Enercon E82 turbines it has been found that it is sufficient to distinguish between two operation conditions (moderate and strong wind).
A key element in the signal analysis is the determination of the standard deviations of the third octave band amplitude modulations (Figure 1). Hereby the relation

$$s^2_{\text{stochastic},i} = s^2_{\text{tot},i} - s^2_{\text{periodic},i} - s^2_{\text{pinknoise},i}, \tag{6}$$

is used where $s_{\text{tot},i}$ denotes the total standard deviation of F_i and $s_{\text{pinknoise},i}$ is the standard deviation of level fluctuations of a reference pink noise signal which is processed in the same manner as the wind turbine signal. In a first step the periodic amplitude modulation is estimated by evaluating the autocorrelation function. In a second step the stochastic amplitude modulation is determined as the unknown variable in Eq. 6.

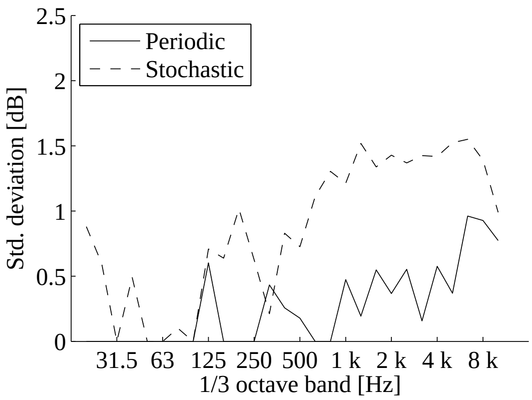

Figure 1: Standard deviations of periodic and stochastic level fluctuations (or AM) of a Vestas V90 at strong wind conditions.

Propagation filter

The propagation filter maps the audio signal generated by the emission synthesizer onto the signal that corresponds to the sound pressure at the receiver position. The corresponding filter function varies over time to account for random fluctuations due to atmospheric turbulence. In the general case of a moving receiver, the Doppler effect is considered by a suitable time dependent mapping scheme that relates the source and receiver time axis. While the filter implementation of geometrical spreading, air absorption and possible barrier attenuation is straightforward, the ground effect and the level fluctuations need a closer look and are discussed in more detail below.

Ground effect

Simulation by a FIR filter

Ground effect is modeled here according to the underlying physical mechanism as interference between direct and ground reflected sound. As a simplification it is assumed that the reflection occurs at an infinitely extended plane defined by the topography at the receiver position. The ground reflection differs from the direct sound by scaling with a complex reflection factor and an additional delay. The ground reflected sound is represented as $F_g(e[k])$ with the filter function F_g:

$$F_g(e[k]) = \frac{r_d}{r_r} \left((e[k] * q[m]) * g_l[m] \right) \tag{7}$$

where $e[k]$ is the k-th sample of the emission signal, r_d is the source - receiver distance, r_r is the distance source - ground reflection point - receiver, $q[m]$ is the impulse response of the spherical wave reflection coefficient Q, $g_l[m]$ is the impulse response of a delay by l samples where $l = \mathsf{round}(f_s \cdot (r_r - r_d)/c)$ with f_s: sampling frequency, c is the speed of sound and $*$ is the discrete convolution operation. q is realized here as FIR filter where the coefficients are obtained by inverse Fourier transformation of $Q(f)$ and subsequent limitation to a length of n taps. The FFT length is chosen as 64 k, corresponding to a frequency resolution $\Delta f = 0.673$ Hz ($f_s = 44.1$ kHz). It is found that for high elevated sources and distances up to 1000 m, approximately 40 taps (n) are sufficient to reproduce the ground effect with an accuracy better than 1 dB.

Source extension

In order to validate the ground effect simulation, several measurements were performed at Mont Crosin, Switzerland over soft ground (grass land). The source was a Vestas V90 turbine with a hub height of 95 m. The receiver was positioned in different distances to the source, firstly close to the ground (0.05 m) and subsequently at a height of 1.60 m. The measurements were evaluated as narrow band spectrum differences between the position at 1.60 m and the 'close to ground' position. For the measured geometries the corresponding level differences were calculated assuming a point source at the hub position. As can be seen in Figure 2, the point source assumption leads to pronounced interference patterns that are not confirmed by the measurements. The relatively weak ground effect dips in the measurements implicate an extension of the source. Indeed this is confirmed by observations of the emission of wind turbines by acoustical cameras [8]. In the following it is assumed that the source has a vertical extension that corresponds to the diameter of the rotor. Corresponding calculations with five different point sources distributed equidistantly in height reproduce the measurements in Figure 2 reasonably well.

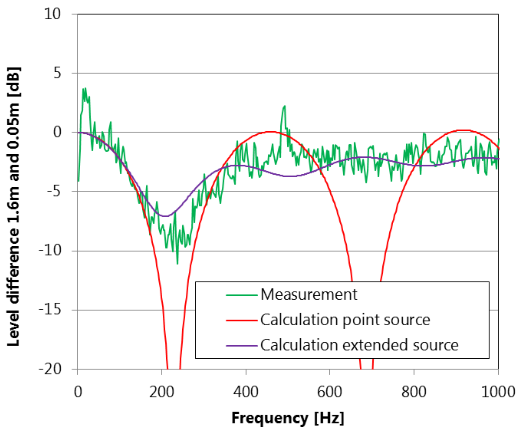

Figure 2: Measured and calculated (point source and extended source assumption) level differences of wind turbine noise evaluated as level differences for a microphone position 1.60 m above ground and close to the ground (0.05 m). The source - receiver distances was 400 m, the height of the nacelle was 95 m, the propagation was over grassy land.

Atmospheric fluctuations

Introduction

During propagation over larger distances, significant sound pressure level and phase fluctuations occur due to temporally varying inhomogeneities of the atmosphere. The two relevant properties of the atmosphere are temperature and wind speed. The major consequence of these fluctuations is a random variation of the level at the receiver, not yet considered is the loss of coherence between direct and ground reflected sound.

Characterization of atmospheric turbulence

The characterization of the fluctuations of the sound propagation speed is usually based on the refraction index n. It can be written as

$$n = 1 + \mu = \frac{c_0 + v_0}{c} \tag{8}$$

where μ is the fluctuating part of the refraction index, c is the momentary effective speed of sound, c_0 is the reference speed of sound in a medium at rest and v_0 is the average wind speed component in propagation direction. In order to further investigate the amplitude fluctuations for the specific case of wind turbine noise propagation, numerical simulations were carried out with a finite difference time domain model (FDTD) developed by Empa.

Numerical simulations

The numerical FDTD simulations made usage of the concept of *frozen turbulence*. Thereby it is assumed that the condition of the atmosphere does not change during a pulse propagation from source to receiver. After many runs with arbitrary fields of the refraction index $n = 1 + \mu(r, z)$ with r: horizontal distance coordinate and z: height, statistical quantities can be derived that yield information about the distance and frequency dependency of the global amplitude fluctuations. The above observation that the source has to be regarded as extended over a height that corresponds to the rotor diameter has to be considered here as well, as this leads to a certain averaging over small-scale local medium inhomogeneities.
The $\mu(r, z)$ fields are realized according to Salomons [9]. However, as the source is high above ground, a height dependent correlation length L is assumed according to $L(z) = 0.3z + \exp(-0.3z)$ with z: height in [m]. Figure 3 shows a $\mu(r, z)$ field realization for turbulence parameters $\sigma_v = 1.3$ m/s, $\sigma_T = 0.3°$C, $c_0 = 340$ m/s, $T_0 = 293$ K and $N = 200$ and $\Delta k = 0.05$ m^{-1}.

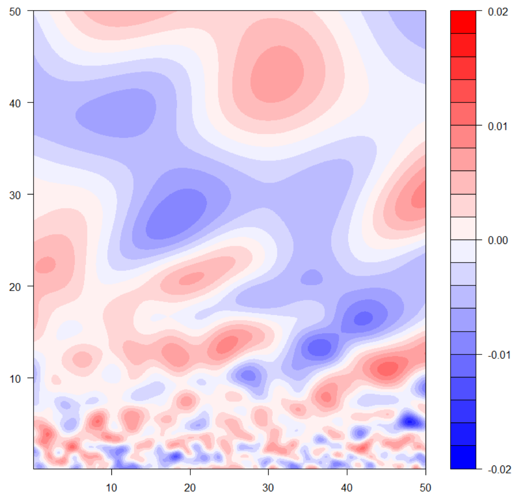

Figure 3: Example of a 2D field of the fluctuating part of the refraction index $\mu(r, z)$. The horizontal axis corresponds to the r coordinate, the vertical axis is z, both in meters.

With the above introduced turbulence parameter values, 14 different $\mu(r, z)$-field realizations (Fig. 3) were determined. For each $\mu(r, z)$-field, the sound propagation was calculated with a FDTD simulation from five different point sources at heights 45 m, 62.5 m, 80 m, 97.5 m and 115 m to four receivers in 100 m, 200 m, 300 m and 400 m at at height of 1.6 m. Figure 4 shows the calculated level fluctuations as a function of frequency for a propagation distance of 400 m. The fluctuations clearly increase with frequency, but show no smooth behavior. This can be attributed to ground effect interferences that lead to abnormal frequency dependent sensitivities with respect to an inhomogeneous atmosphere. The standard deviations for the individual point sources range up to 5 to 7 dB at 1.6 kHz. However if the already mentioned source extension is taken into account and the average of all five point sources is considered, the resulting standard deviation drops to about 2.5 dB at 1.6 kHz which is consistent with measurements. The observations on the ground effect and the magnitude of fluctuations both confirm that a wind turbine has to be modeled as an extended source.

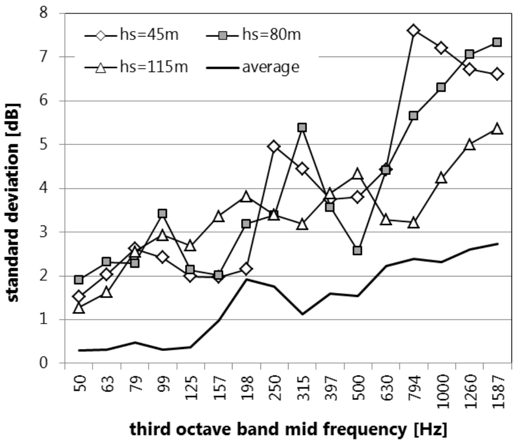

Figure 4: Frequency dependent standard deviations of the fluctuations for a point source at three different heights and the average of all five source positions. The horizontal distance to the receiver is 400 m.

An additional evaluation yielded a high correlation between the individual third octave band fluctuations for bands above 500 Hz. As the fluctuations drop with decreasing frequency, the high-frequency synchronicity is assumed here for the whole frequency range. Consequently the modeling of the fluctuations simplifies to a global, time-varying high-shelf filter function $F_0^t()$ with amplitude response in [dB]:

$$|F_0^t(f)| = (A(t) - C_{\text{off}}) \frac{1}{1 + \exp\left(\frac{\ln(81)}{f_1 - f_2}[f - 0.5(f_2 + f_1)]\right)} \tag{9}$$

where $A(t)$ [dB] is steered by a random process and f_1 and f_2 are the frequencies for which the high-shelf function reaches 10% and 90% of its final value. As $A(t)$ in dB varies equally around 0, an additional offset correction C_{off} is needed to adjust for energy neutral fluctuations. From the numerical simulations the following parameter setting has been derived: $f_1 = 2500/\sqrt{d}$ [Hz] and $f_2 = 20000/\sqrt{d}$ [Hz] with d: horizontal distance between source and receiver in meters. $A(t)$ is adjusted for a distance independent standard deviation of 2.0 dB, considering the fact that the synthesized emission signal that is based on measurements 150 m away from the source, already contains a significant portion of the propagation fluctuation. The random process $A(t)$ is generated by 2 Hz low-pass (order 3) filtered white noise.

Discussion and Conclusions

The quality of the proposed wind turbine auralizator was successfully tested in a preliminary experiment with experienced listeners [10] and can be evaluated by direct comparison of recorded and synthesized sounds: `http://www.visasim.ethz.ch/auralization`. The relative small computational effort necessary for the emission synthesizer and the propagation filter allow for a real-time implementation. A difficulty associated with wind turbine noise is the fact, that its characteristics can vary significantly on a time scale of a fraction of a minute. These variations in average noise and tone levels, as well as in amplitude modulation parameters can not be related to a common global wind measurement at 10 m height but are the effect of local variations in the wind field along the blades. For the propagation filtering module it is planned to refine the ground effect modeling by including incoherence between direct and ground reflected sound. In addition, the time dependencies of the fluctuations will be investigated further.
The next step in the project will be a comprehensive validation of the auralizator by laboratory experiments where people will assess the annoyance associated with wind turbine noise - once with real audio recordings and once with synthesized sounds.

References

[1] M. Manyoky, U. Wissen Hayek, T. M. Klein, R. Pieren, K. Heutschi, A. Grêt-Regamey, Concept for collaborative design of wind farms facilitated by an interactive GIS-based visual-acoustic 3D simulation, Proceedings of Digital Landscape Architecture 2012 at Anhalt University of Applied Sciences.

[2] www.visasim.ethz.ch/index.php

[3] R. Pieren, K. Heutschi, K. Eggenschwiler, Auralization of windturbine noise: Emission Synthesis, Acta Acustica united with Acustica (submitted).

[4] K. Heutschi, R. Pieren, M. Müller, M. Manyoky, U. Wissen Hayek, K. Eggenschwiler, Auralization of Wind Turbines: Propagation Filtering and Vegetation Noise Synthesis, Acta Acustica united with Acustica (submitted).

[5] H. Moller, C. S. Pedersen, Low-frequency noise from large wind turbines, Journal of the Acoustical Society of America **129** (2011) 3727-3744.

[6] J. Forssén, M. Schiff, E. Pedersen, K. Persson Waye, Wind Turbine Noise Propagation over Flat Ground: Measurements and Predictions. Acta Acustica united with Acustica **96** (2010) 735–760.

[7] IEC 61400-11:2008: Wind turbines - Part 11: Acoustic noise measurement techniques (IEC 88/324/CD:2008), 2008.

[8] S. Oerlemans, P. Sijtsma, B.M. Lopez, Location and quantification of noise sources on a wind turbine, Journal of Sound and Vibration **299** (2006) 869-883.

[9] E. Salomons, Computational atmospheric acoustics, Kluwer Academic Publishers, 2001.

[10] M. Müller, R. Pieren, J. Bitzer, Modell zur Synthese akustischer Emissionen von Windturbinen, Proceedings DAGA 2012 at Darmstadt.